Inorg. Chem. **2003**, *42*, 5715–5721

Molecular QCA Cells. 2. Characterization of an Unsymmetrical Dinuclear Mixed-Valence Complex Bound to a Au Surface by an Organic Linker

Zhaohui Li and Thomas P. Fehlner*

Department of Chemistry and Biochemistry, University of Notre Dame, Notre Dame, Indiana 46556

Received December 11, 2002

Utilization of binary information encoded in the charge configuration of quantum-dot cells (the quantum-dot cellular automata, QCA, paradigm) requires surface-bound molecule-sized dots for room temperature operation. Molecular QCA cells are mixed-valence complexes, and the evaluation of a surface-bound unsymmetrical, heterobinuclear, two-dot, Fe–Ru molecular QCA cell is described. The tailed complex, *trans*-[Ru(dppm)$_2$(C≡CFc)(N≡CCH$_2$CH$_2$-NH$_2$)][PF$_6$] (dppm = methylbis(diphenylphosphane), Fc = (η^5-C$_5$H$_5$)Fe(η^5-C$_5$H$_4$)), is covalently modified with the molecular adapter, HS(CH$_2$)$_{10}$COOH, for binding to a Au surface. Preparation and characterization of the films by AFM, XPS, and electrochemical techniques are reported. Cyclic voltammetric techniques are used to assess film growth, coverage and uniformity, effects of thiol diluents on areal densities of the complex, and stabilities of the accessible redox states. Amperometric techniques are used to investigate the efficiency of both chemical and electrochemical oxidation in producing the mixed-valence dication on the surface.

Introduction

Field-coupled molecular quantum-dot cellular automata (QCA) cells are sufficient to support general purpose computing with low power loss, making this novel paradigm one that permits high-density electronic circuits in the nanoscale size regime.[1,2] The concept has been substantiated experimentally at low temperatures but remains to be empirically verified in the molecular size regime where room temperature operation is possible.[3] In the preceding paper,[4] we described the evaluation of the heterobinuclear complex, *trans*-RuCl(dppm)$_2$(C≡CFc) (**1**) (dppm = methylbis(diphenylphosphane), Fc = (η^5-C$_5$H$_5$)Fe(η^5-C$_5$H$_4$)) and its mixed-valence complex [*trans*-RuCl(dppm)$_2$(C≡CFc)][BF$_4$] (**1a**) for use as a two-dot QCA cell.[5] The complex was modified for surface binding by attaching an organic linker. [*trans*-Ru(dppm)$_2$(C≡CFc)(N≡CCH$_2$CH$_2$NH$_2$)][PF$_6$] (**2**) and its mixed-valence complex, [*trans*-Ru(dppm)$_2$(C≡CFc)(N≡CCH$_2$CH$_2$-NH$_2$)][PF$_6$][BF$_4$] (**2a**), were characterized in terms of structure and mixed-valence behavior as unbound entities in solution and the solid state.[4] It was found that the mixed-valence complex possesses a valence-trapped Fe(III)−Ru(II) configuration with properties appropriate for the intended application. Here a description of the characterization of the same two-dot cell when bound as a monolayer on the surface of a solid metal substrate is given. Investigated are questions of (1) surface binding, uniformity, and density; (2) generation of the mixed-valence state on the surface by chemical and electrochemical means (charging of the QCA cell); and (3) chemical stability of both complexes on the surface. These studies confirm that a surface-tethered mixed-valence complex possesses basic properties necessary for molecular electronic applications in the QCA paradigm.

Existing techniques for the construction of monolayer films on electrode surfaces are employed in this work although highly ordered assemblies are not required for our purposes.[6] Techniques used to characterize surface-bound **2** are atomic force microscopy (AFM), X-ray photoelectron spectroscopy (XPS),[7] and electrochemistry.[8] AFM provides information on surface morphology albeit not at sufficient resolution to

* Author to whom correspondence should be addressed. E-mail: Fehlner.1@nd.edu.

(1) Lent, C. S.; Tougaw, P. D.; Porod, W.; Bernstein, G. H. *Nanotechology* **1993**, *4*, 49.
(2) Tougaw, P. D.; Lent, C. S. *J. Appl. Phys.* **1994**, *75*, 1818.
(3) Orlov, A. O.; Amlani, I.; Berstein, G. H.; Lent, C. S.; Snider, G. L. *Science* **1977**, *277*, 928.
(4) Li, Z.; Beatty, A. M.; Fehlner, T. P. *Inorg. Chem.* **2003**, *42*, 5707−5714.
(5) Colbert, M. C. B.; Lewis, J.; Long, N. J.; Raithby, P. R.; White, A. J. P.; Williams, D. J. *J. Chem. Soc., Dalton Trans.* **1997**, 99.
(6) Ulman, A. *An Introduction to Ultrathin Organic Films: From Langmuir-Blodgett to Self-Assembly*; Academic: Boston, 1991.
(7) Carlson, T. A. *Photoelectron and Auger Spectroscopy*; Plenum: New York, 1975.
(8) Bard, A. J.; Faulkner, L. R. *Electrochemical Methods*; Wiley: New York, 2001.

10.1021/ic026255q CCC: $25.00
Published on Web 08/14/2003

identify surface-bound species. XPS provides overall analytical information whereas electrochemistry provides both analytical information on redox active species and data on electronic properties relevant to QCA application. All techniques are well documented in the literature, and the last is particularly applicable to surface films containing redox active sites, e.g., addressing the nature of the coupling and electron transfer rates between a redox center and a metal surface via organic linkers.[9,10]

Despite the practical orientation of this work, both the characterization of electron transfer within molecules, e.g., mixed-valence compounds, and electron transfer at interfaces are of fundamental importance as well.[11,12] The former constitutes an area of long-standing interest, including device applications,[13] whereas the latter is of more recent origin. Work by colleagues has shown that the Creutz−Taube complex adsorbs strongly to SiO_2 and retains its mixed-valence character.[14,15] The present work reports the first example of the electronic manipulation of a mixed-valence complex covalently bound to a surface. The focus is the preparation and characterization of the mixed-valence state in a complex attached to a metal surface by an organic linker with particular attention to properties pertinent to the charging and discharging of the QCA cell. That is, the mixed-valence state must have sufficient lifetime to permit device operation yet must also be discharged periodically to permit device clocking (a method of time labeling for information flowing through a device).[16] A subsequent contribution will describe experiments designed to detect switching, i.e., electron movement between the metal centers of the surface-bound dinuclear complex in its mixed-valence state.

Experimental Section

General. Syntheses were carried out under dry argon using standard Schlenk methods. All procedures were carried out in the dark as much as possible (flasks and NMR tubes were wrapped in aluminum foil). All solvents were distilled prior to use. 11-Mercaptoundecanoic acid (95%), DCC (dicyclohexylcarbodiimide), 1-dodecanethiol (98+%), 1-hexanethiol (95%), 1-hexadecanethiol (95%), tetrabultylammonium tetrafluorobate ($TBABF_4$, 99%), tetrabutylammonium hexafluorophosphate ($TBAPF_6$, 98%), and sodium perchlorate hydrate ($NaClO_4 \cdot xH_2O$) were purchased from Aldrich and used as received. Tetrabutylammonium percholate ($TBAClO_4$) was obtained from Strem. Gold substrates (Evaporated Metal Films Corp., Ithaca, NY) consisted of glass slides coated with 50 Å of titanium and 100 Å of a gold layer. [*trans*-$Ru(dppm)_2(C{\equiv}CFc)(N{\equiv}CCH_2CH_2NH_2)][PF_6]$, **2**, was prepared according to the preceding paper.[4]

IR spectra were recorded on a Perkin-Elmer Paragon 1000 FT-IR spectrometer, and samples were prepared as KBr pellets. NMR spectra were measured on a Varian 300 MHz instrument. Mass spectra (FAB^+) were recorded on a JEOL JMS-AX505HA mass spectrometer from a matrix of *p*-nitrobenzyl alcohol.

Synthesis. [*trans*-$Ru(dppm)_2(C{\equiv}CFc)(N{\equiv}CCH_2CH_2NHC(O)(CH_2)_{10}SH)][PF_6]$, **3**, was synthesized from **2**, $HS(CH_2)_{10}CO_2H$, and DCC in 1:1:1 ratio in CH_2Cl_2 (5 mL, 2 h). The resultant yellow-orange suspension was filtered and the yellow filtrate was dried under vacuum. The yellow-orange powder obtained was washed and recrystallized to give a yellow orange crystalline powder. IR (cm^{-1}): 3422 (N−H), 2100 (C≡N), 2089 (C≡C), 1625 (C═O), 840 cm^{-1} (PF_6^-). ^{31}P ($CDCl_3$): −7.1 (s), −143 ppm (PF_6^-). ^1H ($CDCl_3$): 7.1−7.8 (m, 40 H, Ph), 6.35 (t, 1H, NH) 4.8−5.2(m, 4H, CH_2P), 4.02 (s, 2H, C_5H_4), 3.91 (s, 2H, C_5H_4), 3.78 (s, 5H, C_5H_5), 2.1 (t, 2H, CH_2CH_2N), 1.6 (t, 2H, CH_2CH_2N), some peaks around 1.0−2.5 ppm which correspond to CH_2 chain. FAB^+ (nitrobenzyl alcohol matrix) *m*/*z*: 1346 ($[M - PF_6]^+$), 1078 ($[M - PF_6 - (N{\equiv}CCH_2CH_2NH{-}C(O)(CH_2)_{10}SH)]^+$), 869 ($[M - PF_6 - (N{\equiv}CCH_2CH_2NH{-}C(O)(CH_2)_{10}SH) - (HC{\equiv}CFc)]^+$).

Monolayer Preparation. All glassware used to prepare monolayers was immersed in piranha solution (concentrated H_2SO_4 and 30% H_2O_2 in a 3:1 ratio). ***(WARNING!** Piranha solution should be handled with caution: it has detonated unexpectedly.)* After that, the glassware was rinsed with large amounts of high-purity water. Prior to coating, the gold substrates were washed with high-purity water, MeOH, CH_2Cl_2, and acetone and dried in argon. Monolayers are formed by soaking gold substrates in a 1 mM solution (total concentration of **3** and $CH_3(CH_2)_{11}SH$) in CH_2Cl_2 or acetone for 10 min to 12 h. The samples were then removed from the solution, rinsed with large amounts of CH_2Cl_2, acetone, high-purity water, and MeOH to wash away any physisorbed material, and dried in argon. Oxidation of the film was carried out by dipping the electrode into 1 mM [FcH][PF_6] in CH_2Cl_2 for a time that ranged from 5 to 60 min in a drybox.

Electrochemistry. Cyclic voltammetry (CV) of **3** in CH_2Cl_2 was performed on a BAS Epsilon-EC using a Pt working electrode, Pt-plate counter electrode, and Pt-wire pseudo-reference electrode. Tetrabutylammonium hexafluorophosphate ($TBAPF_6$) (0.1 M) was usually used as the supporting electrolyte. CV and DC potential amperometry (DCPA) measurements of the surface-adsorbed monolayers were performed in a standard electrochemical cell with a Pt-plate counter electrode, a Pt-wire pseudo-reference and the gold working electrode on the same instrument. The electrode area, the geometric area exposed to the solution, was about 1 cm^2 but varied between 0.8 and 1.3 for different experiments. All potentials reported are referenced to the Pt wire pseudo-reference (the ferrocene couple is 0.60 V relative to Pt). The CV measurements of the monolayers were also performed in different solvents (CH_2Cl_2, acetone, H_2O) with different electrolytes ($TBAPF_6$, $TBABF_4$, $TBAClO_4$, and $NaClO_4$) at different scan rates. All experiments were done at room temperature in a dedicated drybox.

XPS Measurements. X-ray photoelectron spectroscopy (XPS) was carried out using a Kratos Analytical ESCA system with Mg Kα radiation at 1253.6 eV. The takeoff angle was fixed at 90°. The binding energies for each peak were referenced to the Au $4f_{5/2}$ peak at 84 eV.

AFM Measurements. Atomic force microscope (AFM) images were obtained with a Dimension 3000 instrument and a Nanoscope III controller (Digital Instruments, Santa Barbara, CA). The microscope was equipped with a standard cantilever tip (Nanosensors, 35 N/m) and was operated in a tapping mode.

(9) Wei, J.; Liu, H.; Dick, A. R.; Yamamoto, H.; He, Y.; Waldeck, D. H. *J. Am. Chem. Soc.* **2002**, *124*, 9591.
(10) Napper, A. M.; Liu, H.; Waldeck, D. H. *J. Phys. Chem. B* **2001**, *105*, 7699.
(11) Demadis, K. D.; Hartshorn, C. M.; Meyer, T. J. *Chem. Rev.* **2001**, *101*, 2655.
(12) Marcus, R. A.; Hush, C. P. *J. Chem. Phys.* **1997**, *106*, 584.
(13) Ward, M. D. *Chem. Soc. Rev.* **1995**, 121.
(14) Varughese, B.; Chellamma, S.; Lieberman, M. *Langmuir* **2002**, *18*, 7964.
(15) Wang, Y. Ph.D. Thesis, University of Notre Dame, South Bend, 2002.
(16) Hennessy, K.; Lent, C. S. *J. Vac. Sci. Technol., B* **2001**, *19*, 1752.

Results and Discussion

Synthesis. 2 has been functionalized with an amine group suitable for binding to a Si surface. This linker permits two methods of binding to the Au surface required for this study. In the first method, a monolayer of carboxylic acid terminated alkanethiol was prepared on a gold substrate and amide coupling of **2** to the carboxylic acid groups attempted. On the basis of cyclic voltammetric (CV) experiments (see below) all attempts to form surface-bound complexes led to low coverages of **2**. Hence, the alternative route, in which the amide link is made before surface binding, was employed (Scheme 1). Coupling promoted with dicyclohexylcarbodiimide produced satisfactory yields of [*trans*-[Ru(dppm)$_2$(C≡CFc)(N≡CCH$_2$CH$_2$NHC(O)(CH$_2$)$_{10}$SH)][PF$_6$], **3**. Characterization by spectroscopic means was satisfactory. An X-ray diffraction study suffered from severe disordering in the region of the long chain but did confirm that **2** had been modified in the manner desired. Films on gold substrates (100 Å of Au on 50 Å of Ti on glass) were formed by immersion in a dilute solution of **3**, with or without additional alkanethiol diluent, for times sufficient to achieve saturated coverage as measured by CV experiments.

AFM Characterization. To obtain information on surface roughness and overall uniformity, substrate samples cleaned for deposition and with bound **3** were examined. Surface roughness was that expected for a gold film on glass (1.0 × 1.0 μm square, rms = 1.3 nm for bare and 1.5 nm for coated samples), and there were no obvious differences between the surface topologies with and without **3** bound to the surface.

XPS Characterization. Films of **3** on Au were surveyed by XPS in order to establish the presence of the tethered compound on the surface. Signal to noise was poor, and poor sample to sample precision led us to rely on the electrochemical measurements for quantitative information. However, some useful qualitative information was generated. First, the expected elements were present in the film but not the substrate before deposition. They were Au, S, N, Fe, Ru, F, and P, consistent with attachment of **3** to the surface. With CH_2Cl_2, but not acetone, a significant Cl signal was also observed and is assumed to be from incomplete solvent removal. Comparing the XPS of the same sample before and after it is subjected to CV analysis shows little change in the element ratios. However, if the applied potential is taken above 1.0 V, thereby destroying electrochemical activity, the element ratios change significantly, consistent with degradation.

Electrochemical Characterization. The CV of **1** in solution exhibits two oxidation waves and corresponding reduction waves on the return sweep. The first is reversible; however, by replacing the Cl ligand with the surface linker of **2**, the second step shows quasi-reversibility.[4] The situation for **3** is illustrated in Figure 1 (Note that all potentials in this paper are given relative to Pt rather than ferrocene with a redox couple 0.60 V more positive than Pt.) This linker has only a small effect on the potential and shape of the first wave. However, the scan to 1.5 V generates a small

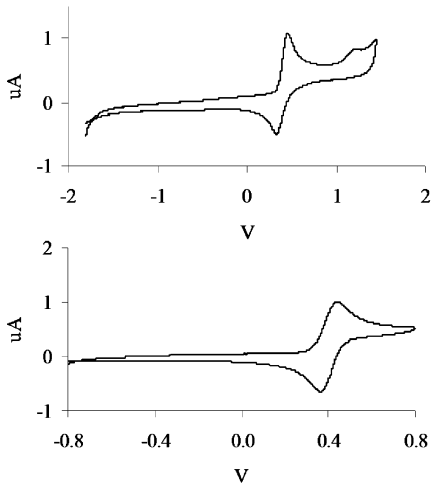

Figure 1. CV of [Ru(dppm)$_2$(C≡CFc)(N≡CCH$_2$CH$_2$NHC(O)(CH$_2$)$_{10}$SH)]-[PF$_6$], **3**, in CH_2Cl_2: (top) first scan from −1.8 to 1.5 V, and (bottom) scan from −0.8 to 0.8 V (vs Pt wire) (0.1 M TBAPF$_6$ in CH_2Cl_2 as electrolyte, scan rate 25 mV/s).

Scheme 1. Preparation of [Ru(dppm)$_2$(C≡CFc)(N≡CCH$_2$CH$_2$NHC(O)(CH$_2$)$_{10}$SH)][PF$_6$], **3**, Bound to a Au Surface

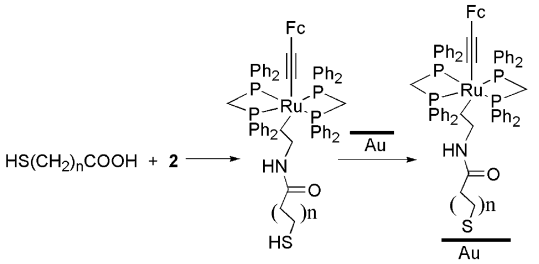

peak at E_{pa} =1.1 V in the first scan. Since the second oxidation of **2** is expected at 1.4 V, this feature may be due to the oxidation of the thiol tail rather than the complex. Indeed the second scan shows nearly no return wave at all at 0.4 V. However, if the scan is limited to 0.8 V, then reversible behavior is observed (E_{pa} = 460 mV and E_{pa} = 340 mV, $E_{1/2}$ = 400 mV).

The CV behavior of **3** bound to a Au surface is shown in Figure 2. If the voltage scan is limited to 0.8 V maximum, then the first wave is reversible: E_{pa} = 134 mV and E_{pc} = 132 mV, E_{fwhm} = 90 mV. E_{pa} and E_{pc} are nearly equal to $E°$, the formal potential. This is the expected situation for strongly bound surface-bound species where the electron transfer from complex to electrode is not rate limiting. Also the peak width is close to the ideal value (90.6 mV) expected for a strongly bound electroactive species.[17] The fact that asymmetric or broad peaks are not observed suggests the presence of isolated, tethered **3** in homogeneous environments relative to redox properties.[18] Note that, compared to **3** in solution, the formal potential has shifted to more negative values. A film deposited from acetone, but measured under the same conditions, has a somewhat higher $E°$ (180 mV) in the same electrolyte and electrode configuration probably due to changes at the Pt wire reference electrode.

(17) Bard, A. J., Ed. *Electroanalytical Chemistry*; Marcel Dekker: New York, 1986.
(18) Auletta, T.; van Veggel, F. C. J. M.; Reinhoudt, D. N. *Langmuir* **2002**, *18*, 1288.

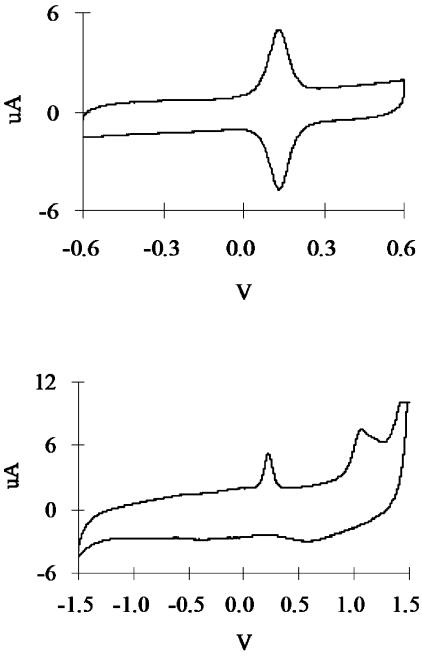

Figure 2. CV for a film in which **3** has been deposited on a Au substrate from a 1 mM solution in CH_2Cl_2 (0.1 M $TBAPF_6$ in CH_2Cl_2 as electrolyte) (scan rate 50 mV/s): (top) scan from − 0.6 V to 0.6 V, and (bottom) scan from −1.5 V to 1.5 V (first scan).

Considering the solution behavior of **3**, it is not a surprise that a sweep to 1.5 V for **3** bound to a Au substrate yields irreversible behavior (Figure 2). In particular, the return scan shows no evidence for the presence of the reducible dication. A second scan shows that the redox activity of the film has been completely destroyed presumably by destruction of the Au−thiol link. The Au−thiol linkage is known to be redox active,[19] and oxidative cleavage of **3** from the surface likely takes place at a lower potential than the second oxidation of the complex.

Integration of the forward or reverse peaks of, e.g., Figure 2 generates the total charge which equals the total number of electroactive tethered complexes **3** on the surface of the electrode. Using the geometric area of the electrode, the surface coverage can be calculated. For saturation coverage of a typical electrode in a solution of pure **3**, an average value of $7.3 \pm 0.7 \times 10^{-11}$ mol cm^{-2}, which corresponds to 230 $Å^2$ per molecule, is obtained for the density of complexes on the surface. A surface roughness factor greater than 1 would reduce the density. Typical polished metal electrodes have roughness factors of 2−3,[17] and from the AFM data a roughness factor for the Au film used can be estimated to be 1.04, a small correction. The structure determination gives a cross-sectional area of **3** of 120 $Å^2$. The area of the $[PF_6]^-$ counterion is 33 $Å^2$, thereby giving a coverage of ≈67%.

The electrochemical method was used to measure coverage as a function of deposition time. The results are given in Figure 3, where it is seen that about 30% of maximum coverage occurs rapidly and that soaking times over 60 min do not appreciably increase the coverage. The coverage of redox active complexes for films prepared with varying

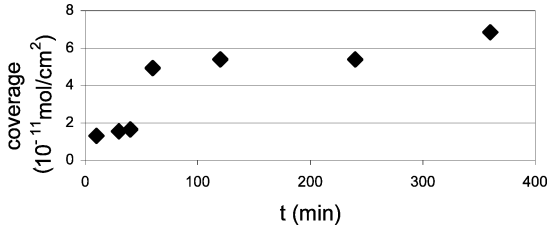

Figure 3. Surface coverage of **3** as a function of the deposition time in a 1 mM solution of **3** in CH_2Cl_2.

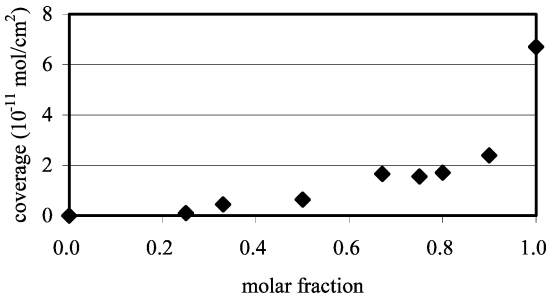

Figure 4. Surface coverage of **3** as a function of the molar fraction of **3** in a mixture of **3** and $CH_3(CH_2)_{11}SH$ with a total concentration of 1 mM in CH_2Cl_2 for 60 min.

amounts of a thiol diluent ($CH_3(CH_2)_{11}SH$) was also examined, and the results are summarized in Figure 4. From the shape of the curve it is evident that the thiol diluent competes preferentially with **3** for the available sites on the surface. Finally, the efficiency of the modified electrode for solution electrochemistry was examined.[20] Similar Au surfaces were examined with no film, with **3**, and with **3** plus added $C_{12}H_{25}$-SH. Under the same conditions, all show reversible CV waves for ferrocene in solution with approximately the same i_p's per unit surface area and similar peak potentials (30 mV average deviation). Although not quantitative, these observations suggest that complex **3** is electrochemically active for ferrocene and that there is not a large complex-free gold surface area exposed to the electrolyte. Indeed **3** should be a good electron transfer match for ferrocene as our studies of complex **3** and related compounds show that the first oxidation takes place on iron.[4]

CV at variable scan rates provides additional information on the nature of the redox behavior of immobilized complexes. The linear dependence of the peak current on the voltage scan rate shown in Figure 5 confirms the presence of strongly surface bound redox centers. Qualitatively similar linear behavior is observed for films deposited in acetone and CH_2Cl_2 albeit with somewhat different slopes. The peak current of an immobilized redox couple is given by $i_p = n^2F^2\upsilon N/4RT$, where n is the number of electrons transferred, F is Faraday's constant, υ is the scan rate, and N is the number of redox active sites on the surface. From Figure 6, $N = 6.24 \times 10^{-11}$ mol for a geometric electrode surface area of 0.84 cm^2 yielding a surface coverage of 7.43×10^{-11} mol cm^{-2} in good agreement with that derived from integration of the charge under the CV curve at a single scan rate. Both methods show that the average area per molecule

(19) Walczak, M. M.; Popenoe, D. D.; Deinhammer, R. S.; Lamp, B. D.; Chung, C.; Porter, M. D. *Langmuir* **1991**, *7*, 2687.

(20) Oh, S.-K.; Baker, L. A.; Crooks, R. M. *Langmuir* **2002**, *18*, 6981.

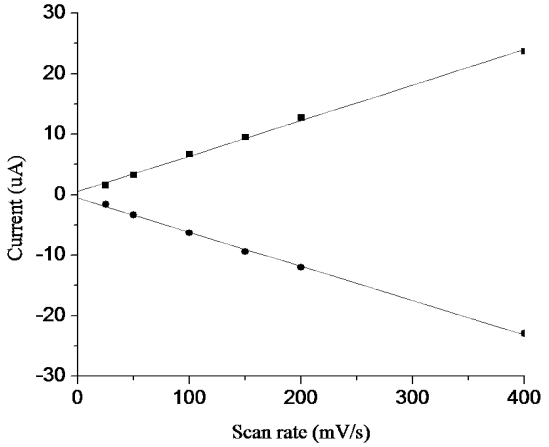

Figure 5. Linear dependence of i_p on the voltage scan rates up to 400 mV/s for a film of **3** deposited on a Au substrate in 1 mM **3** in acetone for 12 h (CH_2Cl_2 with $TBAPF_6$).

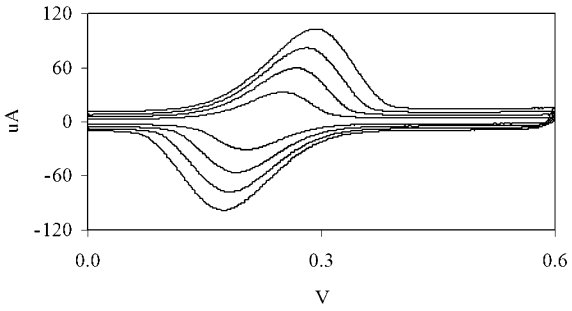

Figure 6. CV of the film described in Figure 5 showing effects of scan rates above 400 mV/s (500, 1000, 1500, and 2000 mV/s) on $E_p - E°$.

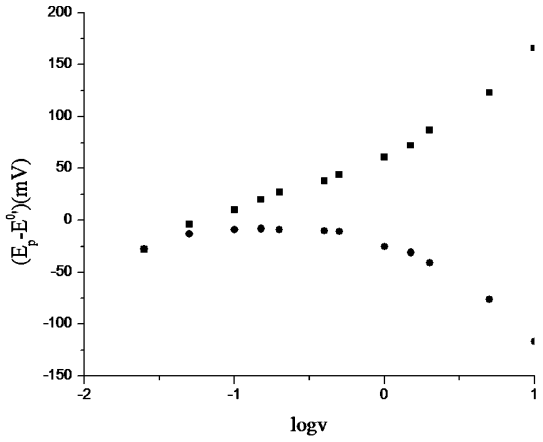

Figure 7. Peak shift from formal potential ($E_p - E°$) vs voltage scan rate for the film described in Figure 5 for the oxidation wave (top) and the reduction wave (bottom).

on the surface is somewhat smaller (higher coverage) in acetone (225 Å^2) than CH_2Cl_2 (282 Å^2).

At higher scan rates (Figure 6) the dependence of the current on scan rates deviates from linearity (see below). The displacement of the maximum of the forward wave from that of the reverse wave occurs when the rate of electron transfer approaches the rate of increase of overpotential.[21] Figure 7 shows a plot of deviation from the formal potential ($E_p - E°$) vs scan rate for both oxidation and reduction waves. Recent work has focused on generating quantitative

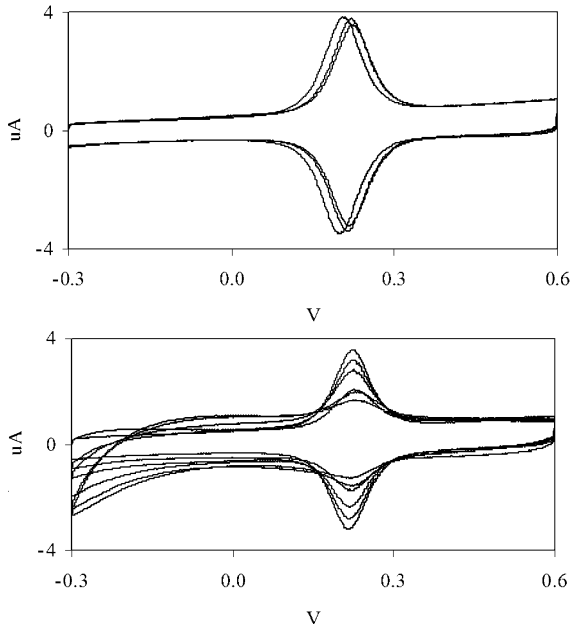

Figure 8. (top) CV of a film of **3** (0.1 M $TBAPF_6$ in CH_2Cl_2 as electrolyte) held at −100 mV for 0, 20, and 80 min showing little change. (bottom) CV of a film of **3** (0.1 M $TBAPF_6$ in CH_2Cl_2 as electrolyte) held at 500 mV for 0 (highest i_p), 10, 30, 70, 110, and 160 (lowest i_p) min showing decrease in i_p and increase in film capacitance with time.

information on, e.g., rate of electron transfer from a tethered complex to the electrode surface as a function of tether length.[22] The films prepared in this work are not ordered, and a distribution of metal complex−electrode distances most likely obtains. Further, these data were not corrected for ohmic drops. Hence, quantitative treatment has not been attempted. However, just as the observation of fluxional behavior in the NMR spectrum generates an order of magnitude rate for the process, so too does the observation of curvature in these ($E_p - E°$) plots. A simple comparison with literature data shows that the rates must be slow (≈10/s) relative to electron exchange in a type II mixed-valence complex.[22] The implication for QCA is that saturated tethers will make substrate-driven clocking rates slow.

Film Performance. For utilization in a device the surface-bound complex must be robust and stable in an operational environment. Hence, we have examined some of the boundary conditions using electrochemistry for analytical measurement. Cycling the film under conditions similar to those for Figure 2 from −0.3 to 0.8 V leads to a loss of maximum current <10% after 40 cycles at a scan rate of 50 mV/s. $E°$ shifts ≈100 mV to positive potential after 40 cycles. Figure 8 shows that holding the film at a negative potential for over an hour causes only minor change in the $E°$ of the wave and a decrease in current of less than 5%. The film is stable under a reduction potential. The situation is different for a positive potential 0.5 V as shown in Figure 8. After only 30 min the peak current has decreased 25% and the charging current, current at low or high potential, has increased substantially. After 160 min i_p is about 15% of its original value. Decomposition of the complex or disruption of its surface bond appears to take place under oxidizing potentials.

(21) Laviron, E. *J. Electroanal. Chem.* **1979**, *101*, 19.

(22) Weber, K.; Creager, S. E. *Anal. Chem.* **1994**, *66*, 3164.

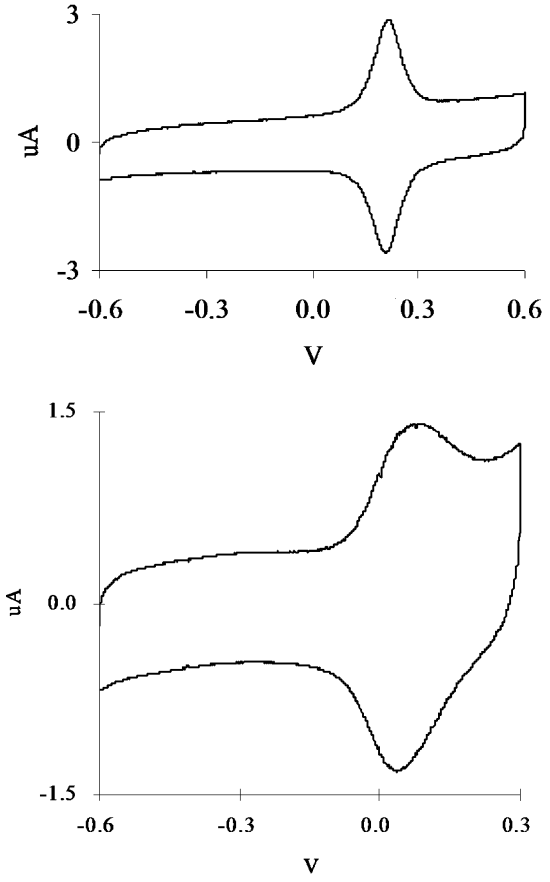

Figure 9. CV of a film of **3** deposited from 1 mM **3** in CH_2Cl_2: (top) 0.1 M $TBAPF_6$ in CH_2Cl_2 as electrolyte, and (bottom) 0.1 M $NaClO_4$ in H_2O as electrolyte.

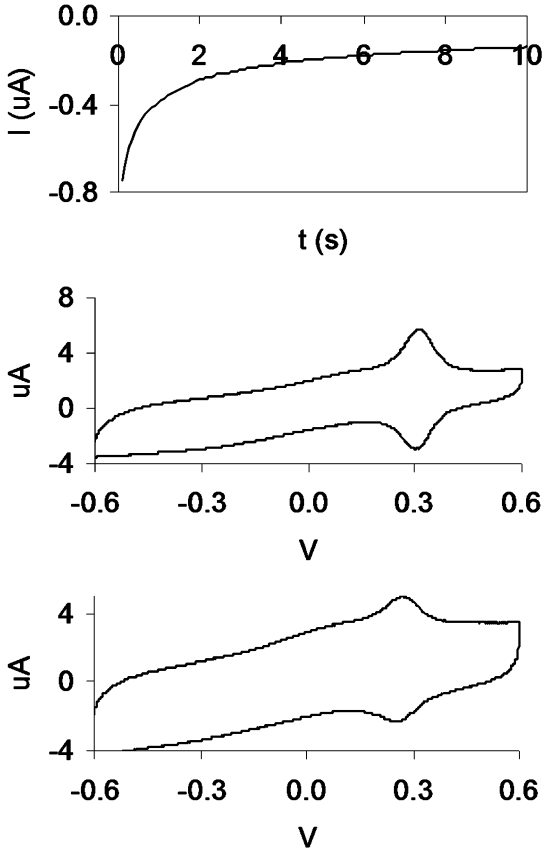

Figure 10. (top) DCPA (50 ms delay time) of a film of **3** after oxidation by 1 mM [FcH][PF_6] in CH_2Cl_2 for 5 min (−100 mV, first scan), (middle) CV of the same film after DCPA reduction demonstrating the presence of surface-bound **3**, and (bottom) CV of the same film chemically oxidized by [FcH][PF_6] and subsequently electrochemically reduced a total of 4 times with varied oxidation times from 5 min to 1 h.

Clearly operation of any QCA device utilizing this particular tailed complex cannot be done at positive resting potentials. On the other hand, the unoxidized film is very robust. After 1 month storage in air, no change in the CV behavior of the film was observed.

Films run in different electrolytes but the same solvent (CH_2Cl_2) show qualitatively similar CV behavior; however, there are quantitative differences. Comparing $TBAPF_6$ with $TBABF_4$ and $TBAClO_4$ shows an increase in fwhm of the wave from a value near the theoretical one to larger values (87, 104, ≈110 mV). $E°$ varies (180, 230, 400 mV), but, as Pt wire is used as the reference, this is most likely due to changes in the reference potential by the supporting electrolyte rather than intrinsic to the mixed-valence state even though it is known that the redox potentials of mixed-valence compounds in solution depend strongly on conditions.[23] If one changes both solvent and counterion, the results shown in Figure 9 are obtained. Switching from $TBAPF_6/CH_2Cl_2$ to $NaClO_4/H_2O$ results in a much broader wave (90 vs 160 mV) and a shift of $E°$ relative to a Pt wire (200 to 40 mV). Considering the fact that **3** is an organometallic complex, operation in a water environment suggests impressive kinetic stability. More importantly, the similar electrochemical behavior in dry solvents vs water suggests that protonation of the surface-bound alkynyl complex to form the vinylidene complex does not take place. Such a reaction would adversely affect the mixed-valence properties. Studies of the electrochemistry of vinylidene vs alkynyl shows the former to exhibit irreversible behavior including spontaneous deprotonation of the oxidized complex to yield observable amounts of the alkynyl complex.[24] Hence, the fact that the electrochemical behavior of **3** in water and nonaqueous solvents is similar shows that protonation is unlikely to occur.

Generation of Films Containing the Mixed-Valence Complex. The goal of this work was the production of stable films containing *trans*-$[Ru(dppm)_2(C{\equiv}CFc)(N{\equiv}CCH_2CH_2NHC(O)(CH_2)_{10}SH]^{2+}$ on gold. Chemical oxidation with excess [FcH][PF_6] for short times was the method of choice. CV of the resulting film shows that the complex remains intact on the electrode (fwhm = 90 mV). Proof of the presence of the oxidized complex was generated with a DC potential amperometric (DCPA) experiment. Application of a reducing potential (Figure 10) shows reduction of surface-bound **3a**, the mixed-valence complex, into **3**. CV analysis shows active complex on the surface. Repeated chemical oxidation followed by DCPA discharge leads to some

(23) Chen, Y. J.; Kao, C.-H.; Lin, S. J.; Tai, C.-C.; Kwan, K. S. *Inorg. Chem.* **2000**, *39*, 189.

(24) Hurst, S. K.; Cifuentes, M. P.; Morrall, J. P. L.; Lucas, N. T.; Whittall, I. R.; Humphrey, M. G.; Asselberghs, I.; Persoons, A.; Samoc, M.; Luther-Davies, B.; Willis, A. C. *Organometallics* **2001**, *20*, 4664.

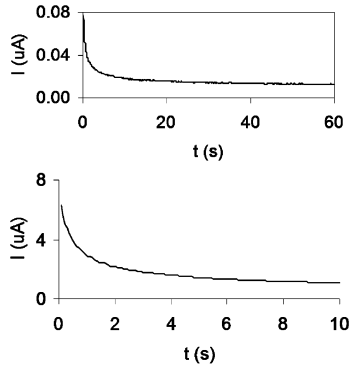

Figure 11. (top) DCPA of a chemically unoxidized film of **3** at −100 mV, and (bottom) DCPA of a chemically unoxidized film of **3** at 500 mV (first scan).

deterioration in the CV signal, but clearly the surface-bound complex survives.

An unoxidized film was subjected to the same amperometric experiment (Figure 11). With a reducing potential, only the small current associated with the electrochemical cell capacitance is observed, whereas with an oxidizing potential a larger current is observed due to electrochemical oxidation of **3** in the film. Comparison of the integrated charges for discharging the chemically oxidized film (0.7 μ C) and charging the unoxidized film (8.6 μ C) (the charge calculated from the oxidizing wave in the CV = 8.0 μ C) gives an overall yield of chemically oxidized complexes on the surface of ≈10%. The origins of the poor chemical yield are not clear. The oxidizing power of chemical reagents depends on conditions,[25] but tethered complexes **3** do not interact strongly, so all should oxidize at the same potential. It may well be a question of accessibility of the surface-bound species to the reagent in solution.

Conclusions

A heterodinuclear metal complex provides stable redox activity within a limited potential range when bound to a gold surface via a thiol linker. Rate of electron transfer between metal complex and metal electrode is relatively slow. The film is stable in a variety of environments including an aqueous one. Chemical oxidation generates a film containing mixed-valence dimers. These results, as well as the electrochemical study, demonstrate that charged, two-dot QCA cells can be bound to a metal surface.

Acknowledgment. We thank Dr. Bindu Varughese for assistance with the XPS experiments, Professor D. Meisel for access to and Dr. Hua Qi for aid with the AFM instrument, and Professors A. G. Lappin and M. Lieberman for helpful advice. The constructive advice of the referees is also appreciated. A grant from ONR/DARPA (N00014-00-1-0746) is gratefully acknowledged.

IC026255Q

(25) Connelly, N. G.; Geiger, W. E. *Chem. Rev.* **1996**, *96*, 877.